TITLE: Heat-induced Maillard reaction of the tripeptide IPP and ribose: Structural characterization and implication on bioactivity

AUTHORS: Zhanmei Jiang, Dilip K. Rai, Paula M. O'Connor, André Brodkorb

NOTICE: This is the author's version of a work that was accepted for publication in *Food Research International*. Changes resulting from the publishing process, such as peer review, editing, corrections, structural formatting, and other quality control mechanisms may not be reflected in this document. Changes may have been made to this work since it was submitted for publication. A definitive version was subsequently published in Food Research International, Volume 50, Issue 1, January 2013, Pages 266-274. DOI: 10.1016/j.foodres.2012.09.028.

Heat-Induced Maillard Reaction of the Tripeptide IPP and Ribose: Structural Characterization and Implication on Bioactivity

Zhanmei Jiang[a], Dilip K. Rai[b], Paula M. O'Connor[c], André Brodkorb[c, *]

[a] Key Laboratory of Dairy Science, Ministry of Education, Northeast Agricultural University, Harbin 150030, China; [b] Teagasc Food Research Centre, Ashtown, Dublin 15, Ireland; [c] Teagasc Food Research Centre, Moorepark, Fermoy, Co. Cork, Ireland

[*]Corresponding Author: Dr. André Brodkorb, Teagasc Food Research Centre, Moorepark, Fermoy, Co. Cork, Ireland. E-mail: andre.brodkorb@teagasc.ie, Tel: +353-(0)25-42222, Fax: +353-(0)25-42340

FINAL revised WORD format Jiang, Rai, O'Connor & Brodkorb, Food Research International (50) 2013

Abstract

Maillard reaction products (MRPs) were prepared from aqueous model mixtures containing 60 g L^{-1} ribose and 30 g L^{-1} of the bioactive tripeptide IPP (Ile-Pro-Pro), heated at 98°C. MRP and associated reactions with changes in IPP were observed within one hour of heat-treatment. The pH of MRPs decreased significantly during the heat treatment of IPP-Ribose mixtures from 9.0 to 7.6 after one hour. The amino group content, IPP and ribose concentration decreased significantly during heat treatment. The fluorescence intensity of the IPP-Ribose MRPs reached the maximum within 2 hours. Modification of the UV/vis spectra for IPP-Ribose MRPs was mainly due to a condensation reaction of IPP with ribose. Compounds with molecular weight between 300 and 650 Da were dominant while compounds smaller than 250 Da were also produced during the reactions, as characterized by size exclusion chromatography. Mass spectrometry revealed that IPP conjugated to ribose at the N-terminal (m/z of 458.3) upon heat-treatment. The presence of ribose also promoted peptide degradation to dehydrated IP (m/z of 211.1). IPP-ribose MRPs lost the known angiotensin-I-converting enzyme (ACE) inhibitory activity of IPP; however, strong antioxidant properties were detected.

Key words: Maillard reaction, IPP, ribose, angiotensin-I-converting enzyme inhibitory activity

1. Introduction

Maillard reaction is a series of complex non-enzymatic browning reactions through condensation of amino groups from amino acids, peptides or proteins and carbonyl groups of reducing sugar (Hodge, 1953; Werner, 1982). Maillard reaction is strongly influenced by some factors such as temperature, pH, time, water activity and reactants type and concentration (Wijewickreme, Kitts, & Durance, 1997). Maillard reaction usually occurs during processing and storage of foods and produces a large number of Maillard reaction products (MRPs) including aroma compounds, ultraviolet absorbing intermediates and brown compounds (Ledl, Beck, Sengl, Osiander, Estendorfer, Severin, et al., 1989).

Recently, several studies were carried out on kinetics (Laroque, Inisan, Berger, Vouland, Dufossé, & Guérard, 2008), antioxidant activity (Guerard & Sumaya-Martinez, 2003; Kim & Lee, 2009a, 2010; Sumaya-Martinez, Thomas, Linard, Binet, & Guerard, 2005; Sun & Luo, 2011), emulsifying properties (Decourcelle, Sabourin, Dauer, & Guerard, 2010) and taste properties (Ogasawara, Katsumata, & Egi, 2006) of Maillard reactions products of amino acids, peptides and proteins. For example, the effect of Maillard reaction temperature on products of xylose-soybean peptide system were studied (Lan, Liu, Xia, Jia, Mukunzi, Zhang, et al., 2010), antioxidant activities of MRPs from glucose-protein hydrolysate (Guerard & Sumaya-Martinez, 2003), sugar-porcine hemoglobin hydrolysate (Sun & Luo, 2011) and fructose/glucose-glycine oligomer (Kim & Lee, 2009b, 2010) model system were reported. However, little work has been conducted on the angiotensin-I-converting enzyme (ACE) inhibitory activity of MRPs derived from peptide and sugar.

It is known that the tripeptide Ile-Pro-Pro (IPP) exhibits strong angiotensin converting enzyme (ACE) inhibitory activity. It has been isolated and identified in sour milk (Nakamura, Yamamoto, Sakai, Okubo, Yamazaki, & Takano, 1995), and antihypertensive effect and mechanism of IPP were verified in spontaneously hypertensive rats (Nakamura, Yamamoto, Sakai, & Takano, 1995; Yamaguchi, Kawaguchi, & Yamamoto, 2009). However, IPP being a peptide, it can also act as a reactant for Maillard reactions during the processing of foods. Heat-treatment is one of the most common precession steps in the foods industry and it is commonly used for food safety purpose, drying, stabilization or inducing functional properties. As food products are generally complex, including proteins/peptides and carbohydrates, Maillard reaction is one of the most frequent side reactions during heating. As functional foods contain bioactive ingredients with desired health-benefits, their stability and bio-functionality throughout processing, storage and gastro-intestinal transit is of utmost

71 importance. It is not evident whether IPP would keep ACE inhibitory activity in the presence of
72 reducing sugars during the Maillard reaction. It is for this reason that in this work the
73 structure/functionality relationship of IPP and its possible MRPs with one of the most reactive reducing
74 sugars, ribose, is examines as a model system. Therefore, the objective of this study was to evaluate the
75 ACE inhibitory activity, structural changes and kinetics of MRPs of IPP and ribose in aqueous model
76 system.
77
78 **2. Materials and methods**
79 **2.1 Materials**
80 Ile-Pro-Pro (IPP, crude product, purity > 60%) was obtained from Biomatik corporation (Cambridge,
81 Ontario, N3H4R7, Canada). Crude IPP was further purified on a Vydac C18 reversed-phase HPLC
82 column (i.d. 22×250 mm, 10μm; cat. no. 218MS1022). The molecular mass of IPP was verified using
83 MALDI -TOF mass spectrometry and pure IPP was pooled and lyophilized (purity > 98%, HPLC
84 grade). D-Ribose, OPA (o-phthaldialdehyde), L-leucine, Potassium ferricyanide(III) powder, 2,2-
85 Diphenyl-1-picryl-hydrazyl (DPPH), sodium dodecyl sulphate (SDS), Ribonuclease, Bacitracin, MSH
86 tetrapeptide, Leu-Try-Met-Arg, Bradykimin, Tyr-Glu, Leu-Phe, Asp-Glu, Hippuryl-Lhisstidyl-L-
87 leucine (Hip-His-Leu), Angiotensin-I-converting enzyme (ACE, EC 3.4.15.1), L-leucine, and
88 trifluoroacetic acid (TFA) were purchased from Sigma-Aldrich Co. (St. Louis, MO, USA). Other
89 reagents were of analytical grade.
90 **2.2 Preparation of Maillard reaction products (MRPs)**
91 IPP and ribose were dissolved in Milli-Q® water at the concentration of 30 g L^{-1} and 60 g L^{-1},
92 respectively. The pH of the solution was adjusted to 9.0 by 4 M NaOH. The solutions were then
93 transferred to sealed screw-top test tubes, and heated in water bath at 98°C. The samples of the heated
94 mixture were removed at different time-intervals and cooled immediately in ice water. Control
95 experiments with only IPP or ribose were also conducted. The pH was measured at 25°C using
96 calibrated pH meter (pH 340i, WTW82362, Weilheim, Germany).
97 **2.3 Determination of ribose, IPP and free amino group content**
98 The free ribose of the samples was measured with HPLC system (Waters 2695 Alliance, Waters Inc.,
99 USA) equipped with 2414 refractive index detector (Waters Inc., USA), using a WATO44355

carbohydrate column (i.d. 4.6×250 mm, 4 μm, Waters, Ireland). The column temperature was 60°C and 50μL of sample were injected into the HPLC system. The mobile phase was 9 mmol L^{-1} H_2SO_4 and eluted at a flow rate of 0.5 mL min^{-1}. Data analysis was performed using Empower Chemstation software.

The concentration of IPP in the samples was determined by reversed-phase HPLC, using a Symmetry C18 column (i.d. 2.1mm ×150mm, 5μm, Waters, USA), detected at 214nm. The mobile phase used for analysis consisted of Milli-Q® water containing 0.1% TFA (solvent A) and 100% acetonitrile containing 0.1% TFA (solvent B). A linear gradient was carried out with from 0 to 100% B in 30 min at a flow rate of 0.2 mL/min. Injection volume was 5 μL. The eluted peaks were detected at 214 nm and 294 nm.

Available free amino groups were quantified by the OPA (o-phthaldiadehyde) method (Church, Swaisgood, Porter, & Catignani, 1983). Briefly, the 30 μL sample was diluted to 12-fold and mixed with 1 mL of OPA reagent. After vortexing and a minimal 5 min delay in the dark at room temperature, the absorbance was recorded at 340 nm against OPA reagent. The blank was determined in the same manner, except that Milli-Q® water was used instead of the sample. Absorbance readings were converted into free amino contents using a calibration curve obtained with L-leucine (0 to 0.5 g L^{-1}). The change in free amino group was expressed as relative concentrations (%) in comparison with the content of non-heated samples.

2.4 Absorption and fluorescence spectroscopy

UV/vis absorption spectra were recorded using a CARY 1 UV-vis spectrophotometer (Alto, CA) with the wavelength ranging from 200 to 800 nm. The IPP-Ribose MRPs were diluted to 120-fold with Milli- Q® water for UV/vis spectra analysis.

Fluorescence spectra of IPP-Ribose MRPs were determined using a Cary Eclipse Fluorescence Spectrometer (Varian, Palo Alto, CA). Samples were diluted to 120-fold with Milli-Q® water. Spectrum of excitation and emission were scanned from 300 to 400 nm and 370 to 600 nm, corresponding to the emission and excitation wavelength set at 420 and 347 nm, respectively. Both of excitation and emission slits were set to 10 nm. The scan rate was 120 nm/min.

2.5 Molecular weight measurement of MRPs

The Molecular weight distribution profiles of samples were estimated by size exclusion chromatography using a series connection column with TSK G 2000 SW (7.5 mm ×60 cm , 10 μm, Japan) fitted to a TSK guard column (7.5 mm × 7.5 cm). 20 μL of samples were injected at the concentration of 2.5 g L^{-1}. And 30 % acetonitrile in 0.1%TFA Milli-Q® water was used as the eluent at a flow rate of 0.5 mL/min. Absorbances were monitored at 214 nm. Ten standards were used bovine serum albumin (67kDa), β-lactoglobulin (18.4kDa), ribonuclease (13.7kDa), bacitraci (1,423Da), MSH tetrapeptide (764.84 Da), Leu-Try-Met-Arg (604.77Da), bradykimin (368.44 Da), Tyr-Glu (310.31Da), Leu-Phe (278.35Da) and Asp-Glu (262.22Da) as M_W calibration standards (log M_W= -0.1335X+7.9725, with retention time, expressed in minutes, R^2=0.987).

2.6 Liquid Chromatography-Mass Spectrometry (LC-MS)

Samples were diluted to 120 fold and prepared in 0.1% formic acid in water. 2 μL of the sample solution was injected into a C18 column (Atlantis T3, i.d. 2.1×100 mm, 3 μm) using the Waters Alliance 2695 HPLC pump (Waters Corp. Milford, USA) interfaced to quadruples Time-Of-Flight mass (Q-TOF). The mobile phase consisted of water containing 0.1% formic acid (solvent A) and acetonitrile containing 0.1% formic acid (Solvent B). Separation of the analyzes was achieved using the gradient: 90% solvent A for first 1 minute followed by 60% solvent B in 8 minutes. Electrospray ionization mass spectrometry analyses were performed on a Q-TOF Premier (Waters Corp., Milford, USA) on a positive ion mode. The capillary voltage and cone voltage were set at 3.0 kV and 30V respectively. Mass spectral data were recorded for a mass range m/z 100 to 1000. For the LC-MS/MS experiments, precursor ions of interested were selected and subjected to collision induced dissociation (CID) using argon as the collision gas with collision energy set at 15 eV. The MS/MS spectral data were recorded for the mass range m/z 50 ~ 600. The mass spectrometer was externally calibrated and a lock mass of m/z 556.2771 was used to carry out the exact mass measurements.

2.7 ACE inhibitory activity

The ACE inhibitory activity assay was measured by the HPLC method, with a modification of the method of Cushman and Cheung (1971). Hip-His-Leu (5.0 mmol L^{-1}) was dissolved in 50mM sodium borate buffer (pH 8.3) containing 0.5 M NaCl. A mixture containing 120μL HHL solution and 20μL of MRPs were preincubated at 37°C for 5 min, 10 μL of ACE solution (100 Units L^{-1}) was then added and the mixture was incubated at 37°C for 60 min. The reaction was stopped by the addition of 150μL of 1M HCl and filtered through 0.45μm filters. Hippuric acid liberated by ACE was determined by RP-

159 HPLC using a Symmetry C18 column 2.1mm i.d.×150mm, 5 μm (Waters, USA) at 25°C. A linear
160 gradient from 0 to 100 % acetonitrile containing 0.1%TFA was applied in 20 min, and then from 100 to
161 0 % acetonitrile containing 0.1%TFA was reached in 2 min. The detection wavelength was set at 228
162 nm and the flow rate was held at 0.2 mL min^{-1}. The injection volume was 40 μL. The percentage of
163 ACE inhibitory activity was calculated as $(A_0-A_1)/A_0\times100\%$, where A_0 is the hippuric acid without the
164 sample and A_1 is the hippuric acid with the sample.

165 **2.8 Determination of ferrous reducing power**

166 The ferrous reducing power of IPP-Ribose MRPs and IPP samples was determined according to the
167 modified method of Chawla, Chander and Sharma (2009). Briefly, 0.1mL of MRPs sample was diluted
168 12-fold and mixed with 0.5 mL of 0.2 mol/L sodium phosphate buffer (pH 6.6) and 0.5 mL of 1%
169 potassium ferricyanide. The reaction mixtures were incubated in a water bath at 50°C for 20 min,
170 followed by addition of 0.5 mL of 10% trichloroacetic acid. The mixtures were then centrifuged at 5,
171 000×g using an Eppendorf 5417R centrifuge (Eppendorf AG, Hamburg, Germany) for 10 min, and 0.5
172 mL of supernatant was blended with 0.5 mL of Milli-Q® water and 0.1mL of 0.1% $FeCl_3$. The reaction
173 mixture was left for 10 min and its absorbance was measured at 700 nm. The results were expressed as
174 absorbance units. Higher absorbance of the reaction mixture indicated greater reducing power.

175 **2.9 2,2-Diphenyl-1-picryl-hydrazyl (DPPH) radical scavenging activity**

176 DPPH radical scavenging activity of the IPP-Ribose MRPs and IPP samples was estimated according
177 to a modified method of Yen and Hsieh (1995). 250 μL of MRP sample was added to 1 mL of a
178 solution of DPPH, freshly prepared daily, at a concentration of 0.1mmol L^{-1} in ethanol. The reaction
179 solution was then shaken vigorously and allowed to stand in the dark at room temperature for 30 min.
180 The mixture was centrifuged at 4,000×g for 10 min. The absorbance of the supernatant of mixtures was
181 recorded at 517 nm. The percentage of DPPH radical scavenging activity was calculated as follows:
182 DPPH radical scavenging activity (%)=$[A_{blank}-(A_{sample}-A_{control})]/A_{blank}\times100\%$
183 Where A_{sample} is the absorbance of samples, $A_{control}$ is the absorbance of ethanol added instead of 0.1
184 mM DPPH and A_{blank} is the absorbance of ethanol added instead of samples.

185 **2.10 Statistical analysis**

186 Experiments between IPP alone and IPP-ribose systems have been carried out three times. Analyses
187 including the determination of pH, free amino group, IPP, ribose, ACE inhibitory activity, reducing

power and DPPH radical scavenging activity were run in at least triplicate. Experimental results were expressed as means ± standard deviation. Analysis of variance (ANOVA) was performed and significant differences among means from triplicate or more by the Duncan's multiple range tests and T-test using the SPSS system software 13.0. UV/vis spectra, fluorescence spectra and GPC measurements were also carried out in triplicates. LC-MS measurements were performed in duplicates.

3. Results and Discussion

3.1. Changes in pH and free amino group content

During Maillard reactions, the pH decreases mainly due to the formation of organic acids, such as acetic acid and formic acid in the intermediate MRPs (Brands & van Boekel, 2002; Chen, Jin, & Chen, 2005; Rufian-Henares, Delgado-Andrade, & Morales, 2006). The consumptions of the N-terminal amino group would notably decrease the pH of IPP-Ribose MRPs. Changes in pH of IPP-Ribose MRPs and IPP as a function of heating time were shown in Fig.1A. According to the results of Fig.1A, there were significant differences of pH between IPP-Ribose MRPs and IPP systems during the different heat treatment ($P<0.05$). The pH of IPP-Ribose MRPs decreased markedly within the first 4 hours, and thereafter pH of IPP-Ribose MRPs decreased slightly up to 8 hours ($P<0.05$). During the Maillard reaction of glycine, diglycine, triglycine and lysine with sugars, the pH frequently decreased as the heating time increased (Kim & Lee, 2009a, 2009b, 2010; Zeng, Zhang, Guan, & Sun, 2011). In addition, pH of IPP system slightly increased up to 6 hours of heat treatment ($P<0.05$), after which no pH change was recorded ($P>0.05$), which would indicate that the release of dipeptide or an amino acid residue from IPP degradation had little or no effect on the pH of the system.

At an early stage of the Maillard reaction, the terminal α-amino groups of peptides or proteins and ε-amino groups of lysine residues react with the carbonyl groups of reducing sugars (Ledl, Beck, Sengl, Osiander, Estendorfer, Severin, et al., 1989; Van Boekel, 1998). The loss of available amino groups is another indicator of the reactivity of Maillard reaction. To assay amino group availability, the quantities of free amino groups in IPP heated in the presence and absence of ribose for up to 8 h were determined using the OPA method and results also shown in the Fig.1A. Consumption of free amino groups of IPP-Ribose MRPs was much larger than that of IPP alone ($P<0.05$). For IPP-Ribose MRPs, the number of free amino groups continuously decreased upon heating time ($P< 0.05$). An overall loss of 84.3% free amino groups was observed after 8 h of heating treatment. This suggested that α-amino groups of IPP were progressively bound to the carbonyl groups. In the shrimp hydrolyses-sugar

systems (55°C), there was consumption of free amino groups throughout the 24 hour of Maillard reaction (Laroque, Inisan, Berger, Vouland, Dufossé, & Guérard, 2008). The disappearance of the free amino groups also occurred in heated bovine serum albumin (BSA)-glucose model systems at pH 8.0 and pH 9.7 (Ajandouz, Desseaux, Tazi, & Puigserver, 2008). In the case of IPP heated alone, the free amino groups decreased slightly up to 6 hours, but the remaining free amino groups significantly changed from 86.1±1.1 % to 59.1±0.4 % for the 6th and 8th hour of heating ($P<0.05$). And this indicated that longer and stronger heat treatment could destroy and consume some amino groups of IPP.

3.2. Consumption of IPP and ribose during heat-treatment

During the Maillard reaction, time dependent changes of IPP and IPP-Ribose MRPs concentrations were determined by RP-HPLC and ribose concentrations in heated solutions of IPP alone and IPP-ribose mixtures by HPLC, shown in the Fig.1B. In the IPP solution heated alone, IPP concentration decreased slowly from 0 to 6h, but decreased significantly from 76.3±0.5 to 53.7±0.1 mmol/L between 6 to 8 hours heating. IPP concentration in IPP-Ribose mixtures decreased more significantly than that from IPP. For example, residual IPP of IPP-Ribose MRPs was reduced to approx. 6% of the initial concentration after 8 hours of heat treatment, but about 58.2% in the IPP heated alone. However, as shown below, the IPP and ribosylated IPP co-elute under the chromatographic conditions used, therefore the given amounts of IPP are overestimated in the case of IPP-ribose mixtures.

Ribose concentration in pure ribose samples decreased slightly from 399.7±0.1 mmol/L to 370.5±2.0 mmol/L during heating, most likely due to caramelisation of ribose. In IPP-Ribose mixtures, most of ribose consumptions occurred within the first 3 hour of reaction and thereafter slower disappearance was observed. After 8 hours of heat treatment of IPP-Ribose mixtures, ribose concentration decreased from 399.6±4.4 to 178.1±5.8 mmol/L (~45%), while IPP concentration of IPP-Ribose MRPs also decreased from 92.4±0.3 to 5.3±0.3 mmol/L (~6%), indicating that available carbonyl groups of the sugar disappeared faster than amino groups of the peptide. Sugar consumption has been previously been a factor to evaluate reactivity in Maillard reactions. Laroque, Inisan, Berger, Vouland, Dufossé and Guérard (2008) reported that among all of sugars involved in Maillard reaction with shrimp hydrolysate, ribose was the most active and decreased siginificantly at 55°C after heat treatment of 6 hours. A sharp decrease in glucose of all MRPs was observed at 100°C for up to 240min of the heating time (Kim & Lee, 2009b). These results show a similar trend to those presented in the present paper. The dissappearance of the reactants IPP and ribose were fitted to the first and higher order decay

248 equation(Kehoe, Wang, Morris, & Brodkorb, 2011). None of the reactions fitted first order decays and
249 only poor fitting was possible according to reaction of higher order. This may be partially due to the
250 complex nature of Maillard reactions but also due to the afore-mentioned less accurate determination of
251 IPPconcentrations by RP-HPLC due to the overlap of the reactant IPP and product ribosylated IPP.

252 **3.3. Absorption spectroscopy**

253 In Maillard reaction, a yellow color appeared in the IPP-Ribose mixture after 1 hours heating,
254 increasing in intensity and change into brown with heating times. In order to detect the possible
255 presence of chromophores formed during the Maillard reaction of IPP with ribose, an absorbance was
256 measured between 200 and 800 nm. Fig. 2A shows the UV/vis spectra of IPP heated in the presence (A)
257 and absence of (A') ribose. IPP showed a maximum of absorbance at 214 nm, corresponding to the
258 absorbance of the peptide bond. Upon Maillard reaction of IPP, a significant increase of the maximum
259 of absorbance at 214 nm was observed for up to 6h, but decreased slightly thereafter. In addition,
260 absorbance spectra changed after 4 hours heating in the spectral region between 240 and 450 nm. And
261 at least two new chromophores, appeared at about 286±7nm (from 1 hour to 4 hour of heating time)
262 and 294±0.5nm (at 6 hour and 8 hour of heating time), respectively. In comparison, MRPs derived
263 from glucose and glycine, diglycine, or triglycine had a maximum absorbance in the range 260nm to
264 320nm (Kim & Lee, 2009b). In contrast to this, glycation of β-lactoglobulin induced the emergence of
265 at least two new chromophores at around 330 and 370 nm (Chevalier, Chobert, Dalgalarrondo, &
266 Haertle, 2001). These studies suggest that chromophores depended on both the amino group origin and
267 types of sugars used. In the present study, the absorbance of the new chromophores increased for up to
268 6 h, but decreased slight at the 8 hours heating, probably due to degradation of the chromophores
269 compounds during advance Maillard reaction. In comparison, IPP heated alone showed no increase of
270 absorbance between 240 and 450 nm and absorbance at 214 nm was almost unchanged up to 6 hours
271 but decreased at the 8 hour heating, most likely due to a loss of IPP (shown in the Fig.2A') and
272 degradation of peptide bond of IPP.

273 **3.4. Fluorescence spectroscopy**

274 During Maillard reactions, the appearance of fluorescent compounds prior to the formation of the
275 visible brown pigments has been reported (Baisier & Labuza, 1992; Patton, 1951). Color intensity is
276 considered an indicator for the advanced stage of the Maillard reaction. Fluorescent spectra has been
277 used for characterization of the Maillard reaction (Matiacevich, Santagapita, & Buera, 2005; Morales &

van Boekel, 1997). A increase in fluorescence intensity was reported for MRP of α-lactalbumin with reducing sugars (Sun, Hayakawa, Puangmanee, & Izumori, 2006) and rice protein-glucose system (Li, Lu, Luo, Chen, Mao, Shoemaker, et al., 2009). In contrast, fluorescence increase was non-linear for heated ribose-casein systems (Jing & Kitts, 2004). In present study, fluorescence excitation and emission spectra of IPP-Ribose MRPs were shown as the function of heating time in the Fig.2B. Fluorescence intensity of IPP-Ribose MRPs was the strongest at excitation wavelength of 347±1 nm and emission wavelength of 420±1 nm. During 8 hours of heat treatment, fluorescence intensity of the IPP-Ribose MRPs reached a maximum fluorescence within the first 2 hours, thereafter by a slow decline, indicating that fluorescence compounds accumulated rapidly and reached a maximum before being converted into brown colored pigments.

3.5. Analysis of size exclusion chromatography and reverse phase HPLC

IPP (Fig.3A) and IPP-Ribose MRPs (Fig.3B and Fig.3C) were monitored by size exclusion chromatography. Molecular weight calibration estimated the dominant fraction as 300 and 650Da while compounds smaller than 250Da were also produced during the reactions. When IPP was heated alone, its concentration decreased and traces of thermal degradation products with a lower molecular weight (component N) was produced with increasing heating times. Figure 3B (IPP-Ribose mixtures) also showed small amounts of larger material produced during heating. Meanwhile, components M and N with small molecular weight occurred and showed rising absorbance at 214 nm with heating times. More of component N was produced in IPP-Ribose mixtures compared to that in IPP alone, which suggested that Maillard reaction accelerated thermal degradation of IPP, which matched the finding of mass spectrometry, discussed below in section 3.6. Simultaneous detection at 294 nm (Fig.3C) allowed the detection of intermediate MRPs, corresponding to compounds O (larger Mw), M and Z (both smaller Mw).

Reversed phase HPLC gave addition information on the peptide distribution during the heating of IPP alone (Fig.3D) and IPP-Ribose mixtures (Fig.3E and Fig.3F). In the pure IPP system, IPP concentration decreased as described above. In addition, two peptide compounds, corresponding to peak1 and peak2, appeared during heating. But, the same smaller peak 1 and larger peak 2, also appeared in the IPP-ribose system. It can be assumed that mixture of peak 1 and peak 2 corresponded to peak N in Fig 3A and B, which originated from a thermal breakdown product of IPP, the exact composition being further discussed below. This seemed to demonstrate that the presence of ribose and subsequent Maillard

reaction increased degradation into smaller break-down products. In addition to peak 1 and peak 2, small amounts of other compounds were formed, which all increased in quantity with increasing heating times, some of which absorb at 214 nm (Fig. 3E), others at 294 nm, which are associated to colored MRPs (Fig. 3F).

3.6. LC-MS analysis

LC-MS analysis (Fig.4A) showed the presence of protonated intact IPP and the ribosylated IPP at *m/z* 326.2 and 458.3, respectively, after the heat-treatment. Both IPP and ribosylated IPP co-elute in RP-HPLC (Fig. 3E) at 10.4 min. Further examination of the conjugated product by tandem mass spectrometry revealed that the N-terminus of the tripeptide was involved in the Maillard reaction and thus further confirming the principle of Maillard reaction (Fig.4B). This is supported by the presence of fragments $y"_1$ (*m/z* 116.1) and $y"_2$ ions (*m/z* 213.1) from the tripeptide (Fig.4B(a)) and the corresponding ribosylated IPP (Fig. 4B(b)) suggesting that no modification occurred from the carboxyl end of the tripeptide; while the presence of a_1 (*m/z* 218.2) and b_2-ion (*m/z* 343.2) further confirmed that the conjugation occurred at the N-terminus of the tripeptide. As illustrated in Fig 4B, the mass of a_1-ion in the IPP-ribose MRP is 132Da heavier than the corresponding a_1-ion from IPP alone MS/MS spectrum; the 132Da corresponds to condensation of ribose to the amino group of the tripeptide. A schematic diagram of the generation of product ions from the ribosylated IPP is proposed in Figure 4C. The LC-MS analysis also illustrated a degradation product of IPP in both IPP and IPP-ribose mixtures after heat-treatment, namely the formation of dehydrated form of the dipeptide IP at *m/z* 211.1 $[M+H]^+$ shown in Figure 4D, both of which co-elute in RP-HPLC at 12.8 min (Fig. 3D and E, peak 2) and size exclusion-HPLC (Fig. 3A and B, peak N) at 46.9 min. This degradation product was confirmed by the MS/MS experiment and the fragment ions were outlined Figure 4D inset, which corresponds to peak 2 (Fig. 3D and E) and peak N (Fig. 3A and B). Meanwhile, it is also assumed that peak 1(Fig. 3D and E) might be PP, which elutes in RP-HPLC at 12.6 min and obtained from thermal degradation of IPP.

3.7. ACE inhibitory activity

In vitro ACE inhibition assay is one of the most recognized test for the selection, separation and identification of antihypertensive peptides derived from protein. However, there are spectrophotometric, HPLC, fluorimetric, radiochemical and capillary electrophoresis methods to measure ACE inhibitory activity (Lopez-Fandino, Otte, & van Camp, 2006). In this work, a modified HPLC method was

337 utilized, which based on the hydrolysis of Hippuryl-His-Leu (HHL) by ACE to hippuric acid (HA) and
338 HL; HA released from HHL was measured by RP-HPLC.
339 ACE inhibitory activity (Fig. 5A) of IPP alone and IPP-Ribose MRPs showed significant differences
340 during heating ($P<0.05$). The activity of IPP alone remained relatively high with a small loss of approx.
341 8.6%, probably due to IPP degradation, as outlined above. In contrast to this, ACE inhibitory activity of
342 IPP-ribose MRPs decreased significantly as the heating time increased ($P<0.05$), from 86.1±0.6% to
343 5.9±3.6%, when heated from 0h to 8h. Rufian-Henares & Morales (2007) demonstrated that food
344 melanoidins from coffee (three roasting degrees), beer, and sweet-wine showed in vitro ACE inhibitory
345 activity. Hwang, Kim, Woo, Lee,and Jeong (2011) reported that some of fructose-amino acid and
346 glucose-amino acid MRPs showed slightly higher ACE inhibitory activity than untreated amino acids.
347 In the present study, the reactant IPP showed a high activity, which is diminished by at least two
348 reactions: ribosylation of the peptide and further MRP as well as the increased degradation of IPP into
349 IP variations in the presence of ribose, as shown by MS analysis.

350 **3.8. Antioxidant property**

351 **3.8.1 DPPH radical scavenging activity**

352 It is recognized that DPPH radicals can be scavenged by MRPs through donation of hydrogen to form a
353 stable DPPH-H form (Matthaus, 2002). Much work has been focused on high antioxidant activity of
354 MRPs in sugar-amino acid, -peptide and -protein model systems. Yen and Hsieh (1995) reported the
355 DPPH radical scavenging activity of xylose-lysine MRPs. Sun and Luo (2011) showed that Maillard
356 reaction products (MRPs) from porcine hemoglobin hydrolysate–sugar model system had DPPH
357 radical scavenging activity. And MRPs from α-lactalbumin and β-lactoglobulin with ribose (Jiang &
358 Brodkorb, 2012) and ultrafiltered MRPs from a casein-glucose model system showed strong DPPH
359 radical-scavenging activity (Gu, Kim, Hayat, Xia, Feng, & Zhang, 2009). In this study, DPPH radical-
360 scavenging activity of IPP-ribose MRPs inscreased significantly as the heating time increased ($P < 0.05$)
361 for the first four hours but leveled off at four to eight hours (Fig. 5B). In contrast to this, heated IPP
362 lacked the DPPH radical-scavenging activity of its corresponding MRPs.

363 **3.8.2 Ferrous reducing power**

364 Besides radical-scavenging activity, reducing power is also an important indictor of antioxidant activity.
365 Hydroxyl groups and pyrrole groups of MRPs may play a important role in reducing activity
366 (Yanagimoto, Lee, Ochi, & Shibamoto, 2002; Yoshimura, Iijima, Watanabe, & Nakazawa, 1997).

Benjakul, Lertittikul, and Bauer (2005) reported MRPs of porcine plasma protein-glucose models possessed reducing power. Zeng, Zhang, Guan, and Sun (2011) showed that reducing power of the Maillard reaction products from psicose was also stronger than that from fructose. Ferrous reducing power of IPP-ribose MRPs increased significantly with the heating time ($P < 0.05$, Fig.5B). There was a rapid increase during the first hour, after which it leveled off. However, it was also shown that there was no reducing power of heated IPP.

4. Conclusion

MRPs of IPP with ribose were prepared under the prolonged, high-temperature treatment in alkali pH, during which pH, free amino group, IPP and free ribose decreased considerably. LC-MS analysis and size exclusion chromatography of IPP-Ribose MRPs system indicated molecular rearrangements and production of new smaller molecules occurred during heat treatment. With the disappearance of intact IPP by Maillard reaction and thermal break-down, a considerable loss ACE inhibitory activity was observed as well as an increase in ferrous reducing power and radical-scavenging activity.

Acknowledgement

The studies were supported by the Innovative Research Team of Higher Education of Heilongjiang Province (2010td11) and Project for National Natural Science Foundation of China (31000801). The work was also supported by the Teagasc Food Research Centre, Moorepark. Dr Joseph Kehoe is acknowledged for his help with the kinetic modeling.

Reference

Ajandouz, E. H., Desseaux, V., Tazi, S., & Puigserver, A. (2008). Effects of temperature and pH on the kinetics of caramelisation, protein cross-linking and Maillard reactions in aqueous model systems. *Food Chemistry, 107*(3), 1244-1252.

Baisier, W. M., & Labuza, T. P. (1992). Maillard browing kinetics in a liquid model system. *Journal of Agricultural and Food Chemistry, 40*(5), 707-713.

Benjakul, S., Lertittikul, W., & Bauer, F. (2005). Antioxidant activity of Maillard reaction products from a porcine plasma protein-sugar model system. *Food Chemistry, 93*(2), 189-196.

Brands, C. M. J., & van Boekel, M. (2002). Kinetic modeling of reactions in heated monosaccharide-casein systems. *Journal of Agricultural and Food Chemistry, 50*(23), 6725-6739.

397 Chawla, S. P.; Chander, R.; Sharma, A. (2009). Antioxidant properties of Maillard reaction products
398 obtained by gamma-irradiation of whey proteins. *Food Chemistry,116* (1), 122-128.
399 Chen, S.-L., Jin, S.-Y., & Chen, C.-S. (2005). Relative reactivities of glucose and galactose in
400 browning and pyruvaldehyde formation in sugar/glycine model systems. *Food Chemistry,*
401 *92*(4), 597-605.
402 Chevalier, F., Chobert, J. M., Dalgalarrondo, M., & Haertle, T. (2001). Characterization of the Maillard
403 reaction products of beta-lactoglobulin glucosylated in mild conditions. *Journal of Food*
404 *Biochemistry, 25*(1), 33-55.
405 Church, F. C., Swaisgood, H. E., Porter, D. H., & Catignani, G. L. (1983). Spectrophotometric assay
406 using o-phthaldialdehyde for determination of proteolysis in milk and isolated milk proteins.
407 *Journal of Dairy Science, 66*(6), 1219-1227.
408 Cushman, D. W., & Cheung, H. S. (1971). Spectrophotometric assay and properties of the angiotensin-
409 converting enzyme of rabbit lung. *Biochemical Pharmacology, 20*(7), 1637-1648.
410 Decourcelle, N., Sabourin, C., Dauer, G., & Guerard, F. (2010). Effect of the Maillard reaction with
411 xylose on the emulsifying properties of a shrimp hydrolysate (Pandalus borealis). *Food*
412 *Research International, 43*(8), 2155-2160.
413 Gu, F.L., Kim, J. M., Hayat, K., Xia, S., Feng, B., & Zhang, X. (2009). Characteristics and antioxidant
414 activity of ultrafiltrated Maillard reaction products from a casein-glucose model system. *Food*
415 *Chemistry, 117*(1), 48-54.
416 Guerard, F., & Sumaya-Martinez, M. T. (2003). Antioxidant effects of protein hydrolysates in the
417 reaction with glucose. *Journal of the American Oil Chemists Society, 80*(5), 467-470.
418 Hodge, J. E. (1953). Dehydrated foods-chemistry of browing reactions in model systems. *Journal of*
419 *Agricultural and Food Chemistry, 1*(15), 928-943.
420 Hwang, I. G., Kim, H. Y., Woo, K. S., Lee, J., & Jeong, H. S. (2011). Biological activities of Maillard
421 reaction products (MRPs) in a sugar-amino acid model system. *Food Chemistry, 126*(1), 221-
422 227.
423 Jiang, Z., & Brodkorb, A. (2012). Structure and antioxidant activity of Maillard reaction products from
424 α-lactalbumin and β-lactoglobulin with ribose in an aqueous model system. *Food*
425 *Chemistry,133*(3), 960-968.

426 Jing, H., & Kitts, D. D. (2004). Chemical characterization of different sugar-casein Maillard reaction
427 products and protective effects on chemical-induced cytotoxicity of Caco-2 cells. *Food and*
428 *Chemical Toxicology*, *42*(11), 1833-1844.
429 Kehoe, J., Wang, L., Morris, E., & Brodkorb, A. (2011). Formation of Non-Native β-Lactoglobulin
430 during Heat-Induced Denaturation. *Food Biophysics*, *6*(4), 487-496.
431 Kim, J. S., & Lee, Y.-S. (2009a). Antioxidant activity of Maillard reaction products derived from
432 aqueous glucose/glycine, diglycine, and triglycine model systems as a function of heating time.
433 *Food Chemistry*, *116*(1), 227-232.
434 Kim, J. S., & Lee, Y.-S. (2009b). Study of Maillard reaction products derived from aqueous model
435 systems with different peptide chain lengths. *Food Chemistry*, *116*(4), 846-853.
436 Kim, J. S., & Lee, Y.-S. (2010). Characteristics and Antioxidant Activity of Maillard Reaction Products
437 from Fructose-glycine Oligomer. *Food Science and Biotechnology*, *19*(4), 929-940.
438 Lan, X., Liu, P., Xia, S., Jia, C., Mukunzi, D., Zhang, X., Xia, W., Tian, H., & Xiao, Z. (2010).
439 Temperature effect on the non-volatile compounds of Maillard reaction products derived from
440 xylose-soybean peptide system: Further insights into thermal degradation and cross-linking.
441 *Food Chemistry*, *120*(4), 967-972.
442 Laroque, D., Inisan, C., Berger, C., Vouland, É., Dufossé, L., & Guérard, F. (2008). Kinetic study on
443 the Maillard reaction. Consideration of sugar reactivity. *Food Chemistry*, *111*(4), 1032-1042.
444 Ledl, F., Beck, J., Sengl, M., Osiander, H., Estendorfer, S., Severin, T., & Huber, B. (1989). Chemical
445 pathways of the Maillard reaction. *Progress in Clinical and Biological Research*, *304*, 23-42.
446 Li, Y., Lu, F., Luo, C., Chen, Z., Mao, J., Shoemaker, C., & Zhong, F. (2009). Functional properties of
447 the Maillard reaction products of rice protein with sugar. *Food Chemistry*, *117*(1), 69-74.
448 Lopez-Fandino, R., Otte, J., & van Camp, J. (2006). Physiological, chemical and technological aspects
449 of milk-protein-derived peptides with antihypertensive and ACE-inhibitory activity.
450 *International Dairy Journal*, *16*(11), 1277-1293.
451 Matiacevich, S. B., Santagapita, P. R., & Buera, M. P. (2005). Fluorescence from the Maillard reaction
452 and its potential applications in food science. *Critical Reviews in Food Science and Nutrition*,
453 *45*(6), 483-495.
454 Matthaus, B. (2002). Antioxidant activity of extracts obtained from residues of different oilseeds.
455 *Journal of Agricultural and Food Chemistry*, *50*(12), 3444-3452.

456 Morales, F. J., & van Boekel, M. (1997). A study on advanced Maillard reaction in heated casein/sugar
457 solutions: Fluorescence accumulation. *International Dairy Journal, 7*(11), 675-683.
458 Nakamura, Y., Yamamoto, N., Sakai, K., Okubo, A., Yamazaki, S., & Takano, T. (1995). Purification
459 and Characterization of Angiotensin I-Converting Enzyme Inhibitors from Sour Milk. *Journal*
460 *of Dairy Science, 78*(4), 777-783.
461 Nakamura, Y., Yamamoto, N., Sakai, K., & Takano, T. (1995). Antihypertensive effect of sour milk
462 and peptides isolated from It that are inhibitors to angiotensin-I-converting enzyme. *Journal of*
463 *Dairy Science, 78*(6), 1253-1257.
464 Ogasawara, M., Katsumata, T., & Egi, M. (2006). Taste properties of Maillard-reaction products
465 prepared from 1000 to 5000Da peptide. *Food Chemistry, 99*(3), 600-604.
466 Patton, A. R. (1951). Paper chromatography of browning reaction fluorogens. *Nature, 167*(4245), 406-
467 406.
468 Rufian-Henares, J. A., Delgado-Andrade, C., & Morales, F. J. (2006). Occurrence of acetic acid and
469 formic acid in breakfast cereals. *Journal of the Science of Food and Agriculture, 86*(9), 1321-
470 1327.
471 Rufian-Henares, J. A., & Morales, F. J. (2007). Angiotensin-I converting enzyme inhibitory activity of
472 coffee melanoidins. *Journal of Agricultural and Food Chemistry, 55*(4), 1480-1485.
473 Sun, Y., Hayakawa, S., Puangmanee, S., & Izumori, K. (2006). Chemical properties and antioxidative
474 activity of glycated [alpha]-lactalbumin with a rare sugar, d-allose, by Maillard reaction. *Food*
475 *Chemistry, 95*(3), 509-517.
476 Sun, Q., & Luo, Y. (2011). Effect of Maillard reaction conditions on radical scavenging activity of
477 porcine haemoglobin hydrolysate-sugar model system. *International Journal of Food Science*
478 *and Technology, 46*(2), 358-364.
479 Sumaya-Martinez, M. T., Thomas, S., Linard, B., Binet, A., & Guerard, F. (2005). Effect of Maillard
480 reaction conditions on browning and antiradical activity of sugar-tuna stomach hydrolysate
481 model system. *Food Research International, 38*(8-9), 1045-1050.
482 Van Boekel, M. A. J. S. (1998). Effect of heating on Maillard reactions in milk. *Food Chemistry, 62*(4),
483 403-414.
484 Werner, B. (1982). Chemical changes in food by the maillard reaction. *Food Chemistry, 9*(1-2), 59-73.

485 Wijewickreme, A. N., Kitts, D. D., & Durance, T. D. (1997). Reaction conditions influence the
486 elementary composition and metal chelating affinity of nondialyzable model Maillard reaction
487 products. *Journal of Agricultural and Food Chemistry, 45*(12), 4577-4583.
488 Yamaguchi, N., Kawaguchi, K., & Yamamoto, N. (2009). Study of the mechanism of antihypertensive
489 peptides VPP and IPP in spontaneously hypertensive rats by DNA microarray analysis.
490 *European Journal of Pharmacology, 620*(1-3), 71-77.
491 Yanagimoto, K., Lee, K.-G., Ochi, H., & Shibamoto, T. (2002). Antioxidative activity of heterocyclic
492 compounds formed in Maillard reaction products. In S. T. N. H. F. K. T. Horiuchi & T. Osawa
493 (Eds.), *The Maillard reaction in food chemistry and medical science: Update for the*
494 *postgenomic era*, (pp. 335-340).
495 Yoshimura, Y., Iijima, T., Watanabe, T., & Nakazawa, H. (1997). Antioxidative effect of Maillard
496 reaction products using glucose-glycine model system. *Journal of Agricultural and Food*
497 *Chemistry, 45*(10), 4106-4109.
498 Yen, G. C., & Hsieh, P. P. (1995). Antioxidative activity and scavenging effects on active oxygen of
499 xylose-lysine Maillard reaction products. *Journal of the Science of Food and Agriculture,*
500 *67*(3), 415-420.
501 Zeng, Y., Zhang, X., Guan, Y., & Sun, Y. (2011). Characteristics and Antioxidant Activity of Maillard
502 Reaction Products from Psicose-Lysine and Fructose-Lysine Model Systems. *Journal of Food*
503 *Science, 76*(3), C398-C403.

Fig.1. (A) Changes in pH during heating of IPP-ribose mixtures (▲) and IPP alone (△). Free amino group content of IPP-ribose mixtures (■) and IPP alone (□) during heat treatment at 98°C for up to 8 hours. (B) Time dependent changes of IPP/ IPP-Ribose MRPs concentrations determined by RP-HPLC in heated solutions of IPP alone (△) and IPP-ribose mixtures (▲). Ribose concentration in heated solutions of ribose alone (□) and IPP-ribose mixtures (■). Error bars represent the standard deviation of the mean of triplicate experiments.

Fig. 2. UV/vis absorbance spectra of IPP-Ribose system (A) and IPP (A′) during heat treatment at 98°C up to 8 hours; (B) Fluorescence excitation and emission spectra of IPP-Ribose system; Emission wavelength for excitation spectra was 420nm (scanning from 300 to 400nm). The excitation wavelength for emission spectra was 347nm (scanning from 360 to 600nm). (B′) Fluorescence intensity at emission wavelength of 420nm and excitation wavelength of 347nm.

Fig. 3. Size exclusion chromatograms of IPP at 214nm (A), IPP-Ribose MRPs at 214nm (B) and 294nm (C) during heating (98°C) for different times (from 0 to 8h) at pH 9.0 and corresponding reversed phase HPLC chromatograms of IPP at 214nm (D), IPP-Ribose MRPs at 214nm (E) and 294nm (F) during heating (98°C).

Fig. 4. (A) Electrospray mass spectrum showing the $[M+H]^+$ ions of IPP and ribosylated IPP after 1 h of heating time. (B) CID mass spectra showing the fragment ions of (a) IPP and (b) ribosylated IPP. The spectra shows similar y”1 and y”2-ions while the presence of m/z 218.2 and m/z 343.2 in (b) revealed that the conjugation occurred at the N-terminus of the tripeptide. Schematic diagram (C) shows the point of fragmentation assigned in figure (B). Also the mass peaks marked with * further supports that the conjugation occurred at the N-terminus. (D) Peak corresponded to *m/z* 211.1 in the mass spectrometry analysis and was assigned as the dehydrated dipeptide IP. The dipeptide was confirmed by the MS/MS analysis on the *m/z* 211.1 and the fragment ions were assigned (D inset).

Fig. 5. (A) ACE inhibitory activity during heating of IPP-ribose mixtures (▲) and IPP alone (△). (B) DPPH radical scavenging activity during heating of IPP-ribose mixtures (▲) and IPP alone (△). Ferrous

529 reducing power of IPP-ribose mixtures (■) and IPP alone (□) during heat treatment at 98°C for up to 8

530 hours; Error bars represent the standard deviation of the mean of triplicate experiments.

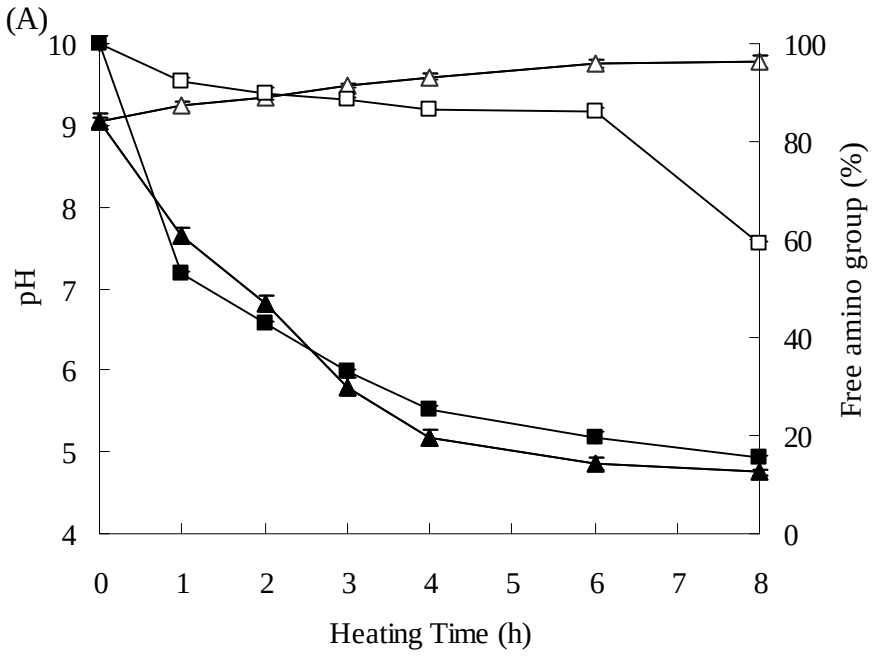

531

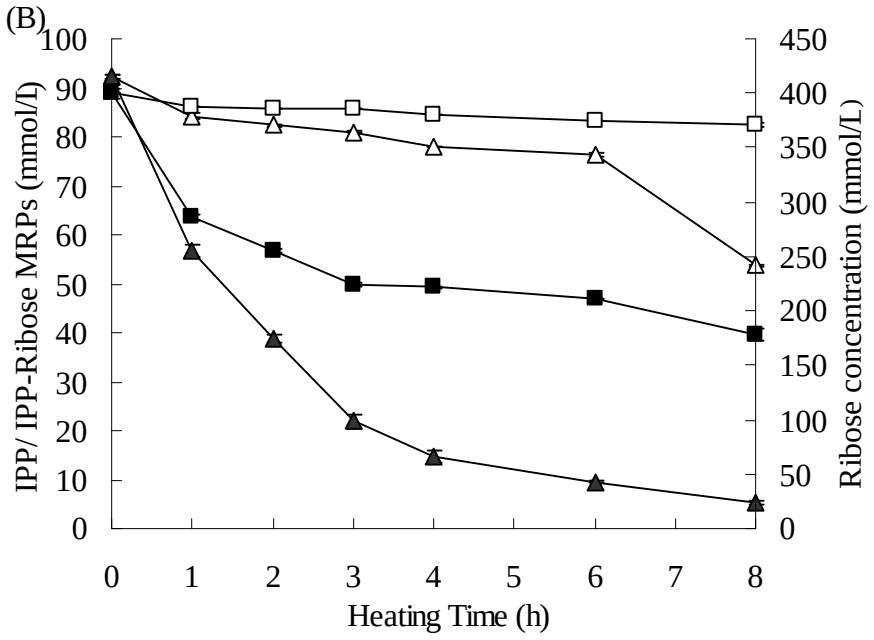

532

533 Fig.1. (A) Changes in pH during heating of IPP-ribose mixtures (▲) and IPP alone (△). Free amino

534 group content of IPP-ribose mixtures (■) and IPP alone (□) during heat treatment at 98°C for up to 8

535 hours. (B) Time dependent changes of IPP/ IPP-Ribose MRPs concentrations determined by RP-HPLC

536 in heated solutions of IPP alone (△) and IPP-ribose mixtures (▲). Ribose concentration in heated

537 solutions of ribose alone (□) and IPP-ribose mixtures (■). Error bars represent the standard deviation of

538 the mean of triplicate experiments.

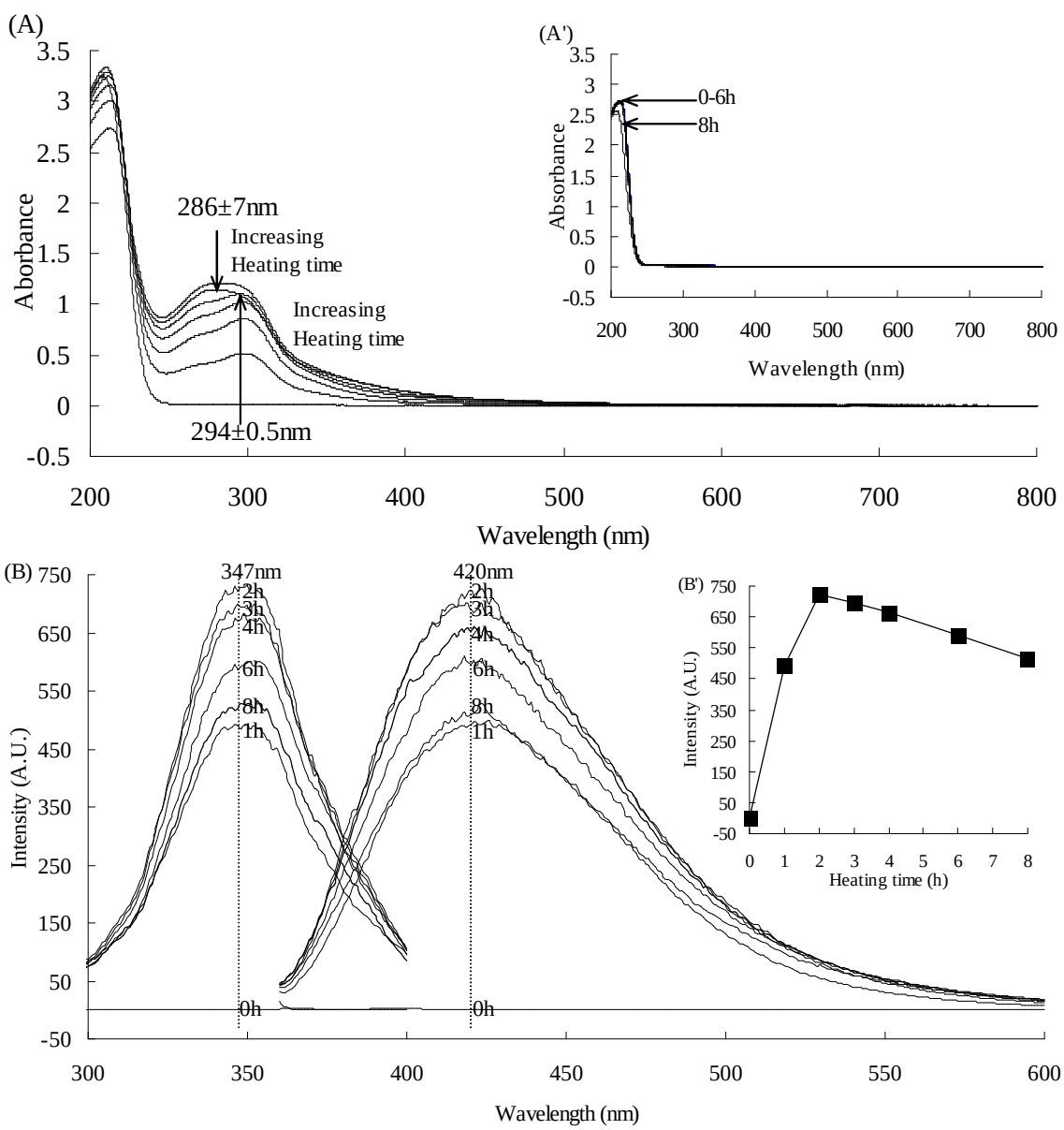

Fig. 2. UV/vis absorbance spectra of IPP-Ribose system (A) and IPP (A′) during heat treatment at 98°C up to 8 hours; (B) Fluorescence excitation and emission spectra of IPP-Ribose system; Emission wavelength for excitation spectra was 420nm (scanning from 300 to 400nm). The excitation wavelength for emission spectra was 347nm (scanning from 360 to 600nm). (B′) Fluorescence intensity at emission wavelength of 420nm and excitation wavelength of 347nm.

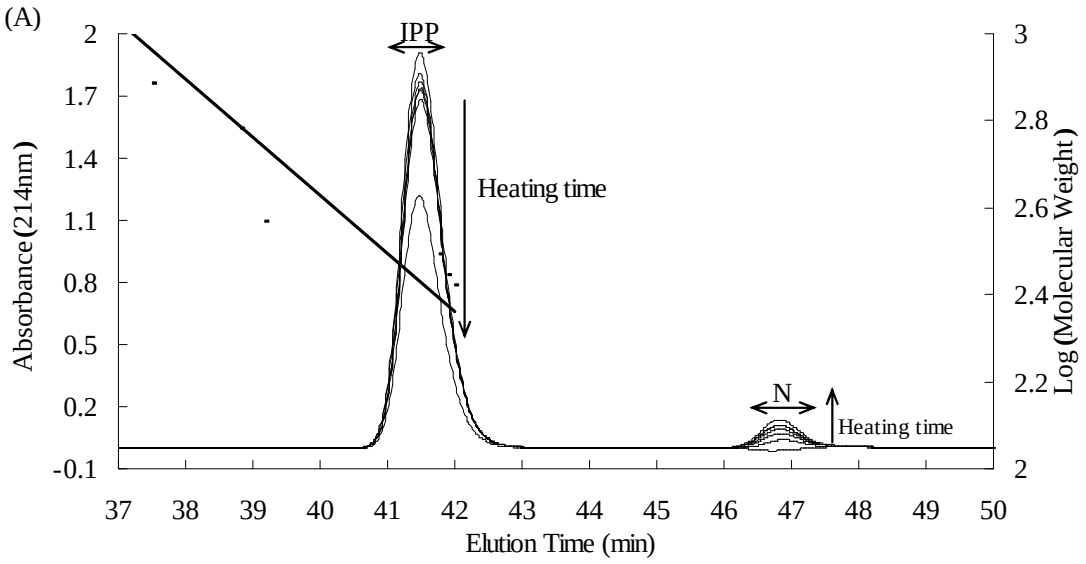
(A)
IPP
Heating time
N
Heating time
Absorbance (214nm)
Log (Molecular Weight)
Elution Time (min)

553

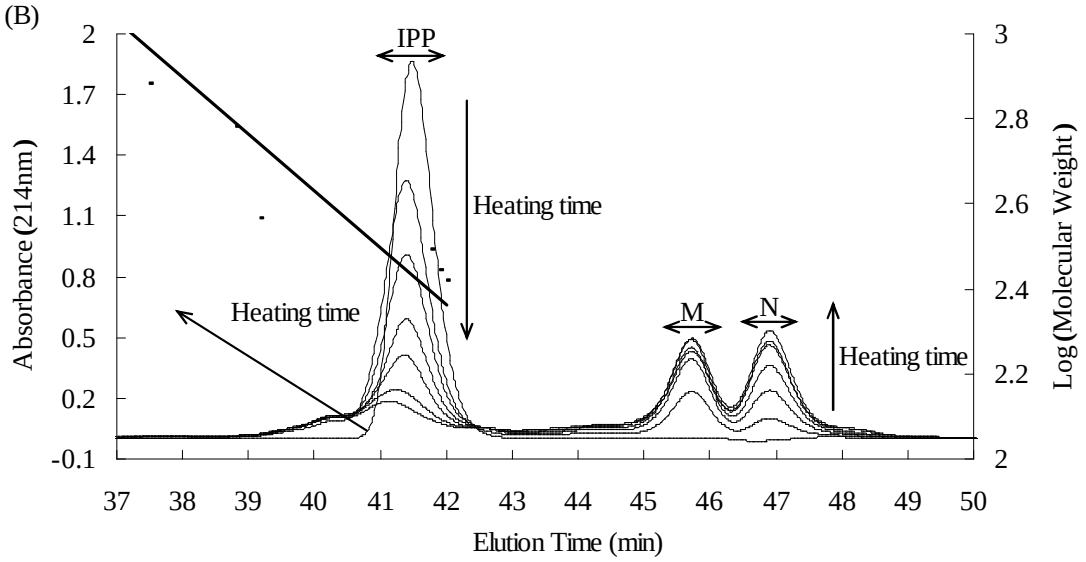
(B)
IPP
Heating time
Heating time
M
N
Heating time
Absorbance (214nm)
Log (Molecular Weight)
Elution Time (min)

554

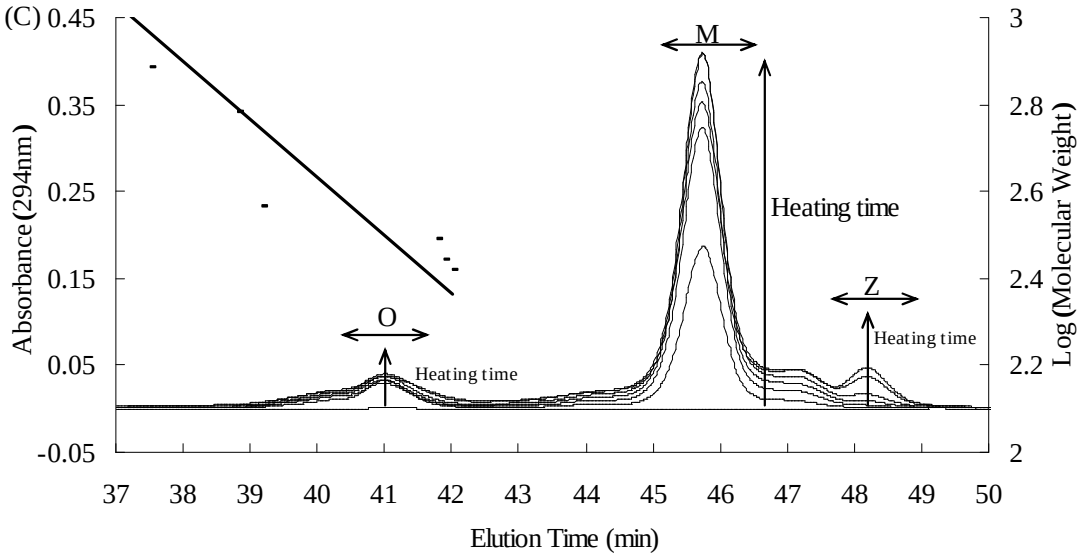
(C)
M
Heating time
Z
Heating time
O
Heating time
Absorbance (294nm)
Log (Molecular Weight)
Elution Time (min)

555

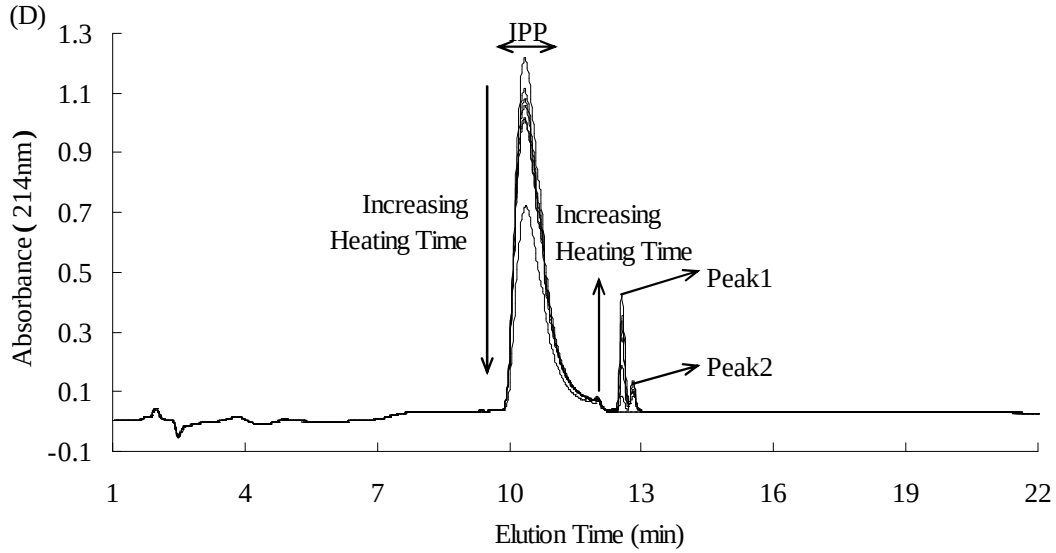
(D)
IPP
Increasing
Heating Time
Increasing
Heating Time
Peak1
Peak2
Absorbance (214nm)
Elution Time (min)

556

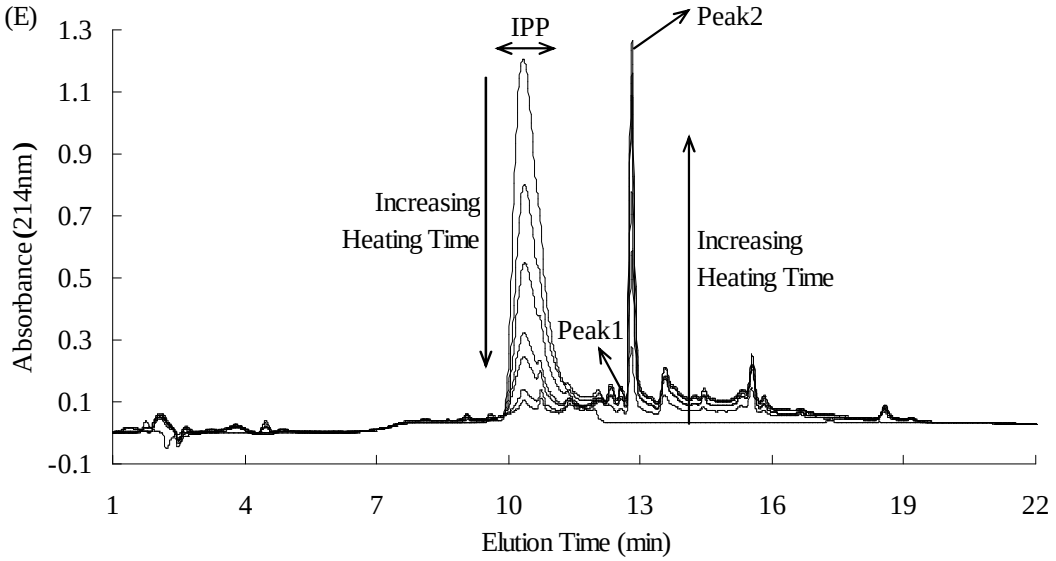
(E)
IPP
Peak2
Increasing
Heating Time
Increasing
Heating Time
Peak1
Absorbance (214nm)
Elution Time (min)

557

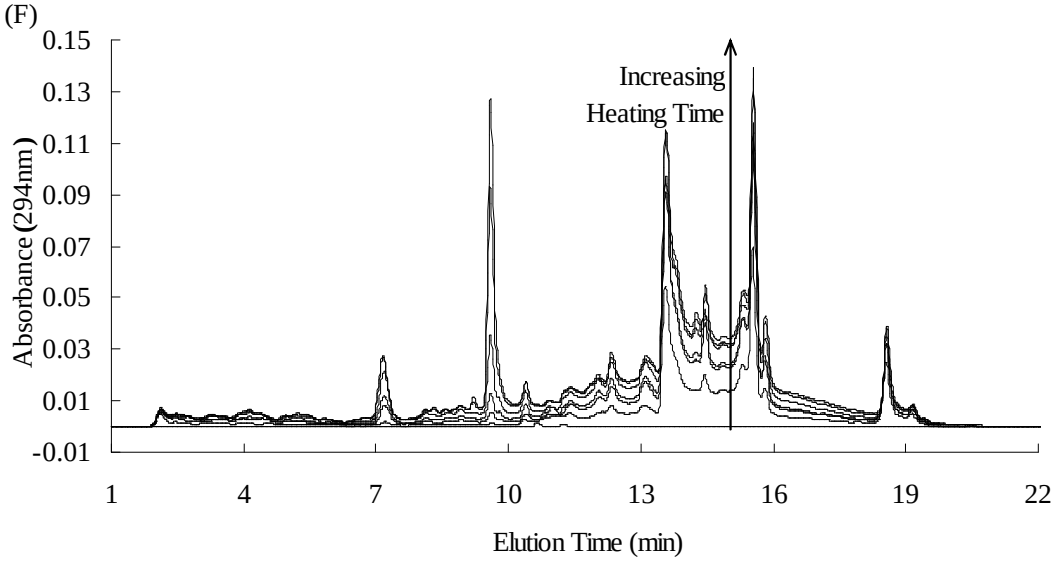
(F)
Increasing
Heating Time
Absorbance (294nm)
Elution Time (min)

558

559 Fig. 3. Size exclusion chromatograms of IPP at 214nm (A), IPP-Ribose MRPs at 214nm (B) and
560 294nm (C) during heating (98°C) for different times (from 0 to 8h) at pH 9.0 and corresponding
561 reversed phase HPLC chromatograms of IPP at 214nm (D), IPP-Ribose MRPs at 214nm (E) and
562 294nm (F) during heating (98°C). Peak description: peak M and Z - small M_w intermediate MRPs; peak
563 O – large M_W compounds; peak 1- dipeptide PP ; peak 2 - dehydrated form of the dipeptide IP at *m/z*
564 211.1 $[M+H]^+$; peak N – mixture of PP and IP.

(A)

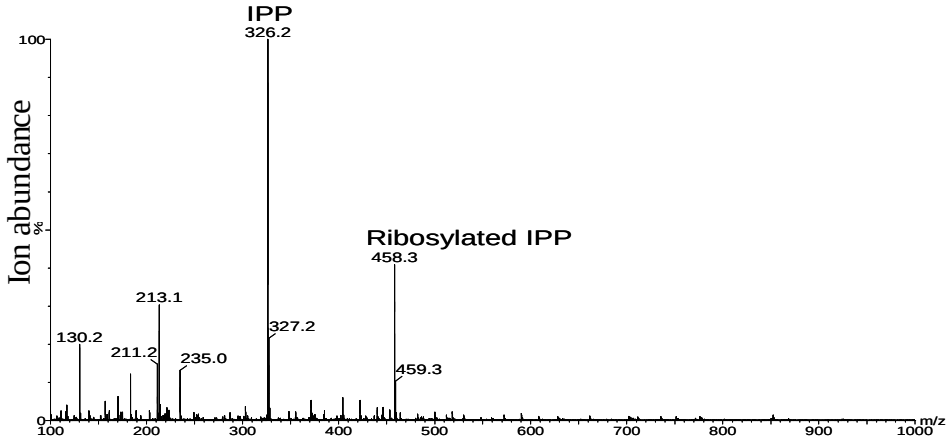
IPP
326.2
Ribosylated IPP
458.3
Ion abundance
%
213.1
130.2
211.2
235.0
327.2
459.3
m/z

(B)

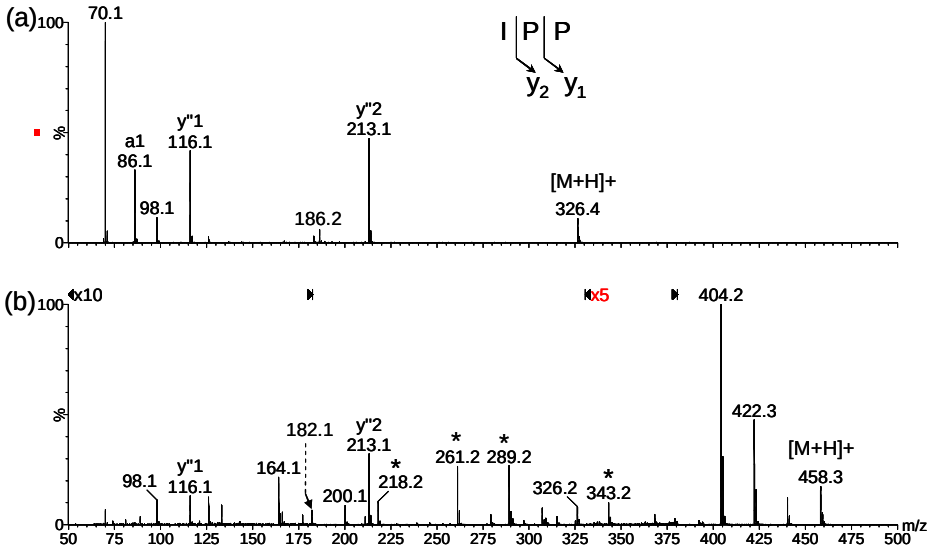
(a)
70.1
I P P
y2 y1
y"1
116.1
a1
86.1
y"2
213.1
98.1
186.2
[M+H]+
326.4
(b)
x10
x5
404.2
422.3
[M+H]+
458.3
182.1
y"2
213.1
y"1
116.1
98.1
164.1
200.1
218.2
261.2
289.2
326.2
343.2
m/z

(C)

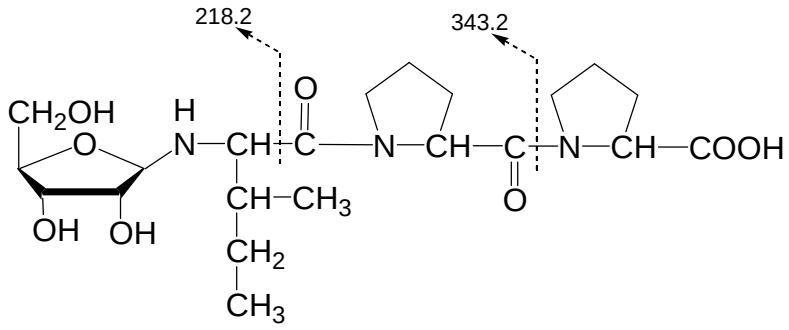
218.2
343.2
CH2OH
O
OH
OH
H
N
CH
C
O
CH
CH3
CH2
CH3
N
CH
C
O
N
CH
COOH

(D)

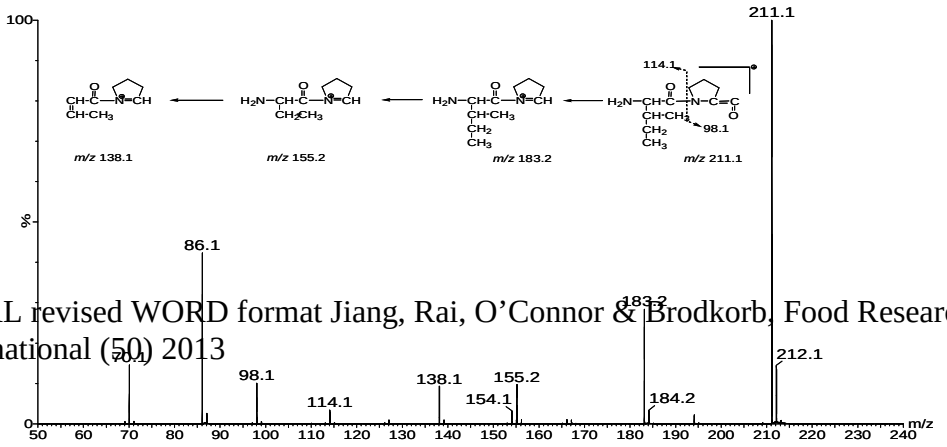
211.1
m/z 138.1
m/z 155.2
m/z 183.2
m/z 211.1
114.1
98.1
%
86.1
183.2
212.1
70.1
98.1
114.1
138.1
155.2
154.1
184.2
m/z

590

591 Fig. 4. (A) Electrospray mass spectrum showing the $[M+H]^+$ ions of IPP and ribosylated IPP after 1 h
592 of heating time. (B) CID mass spectra showing the fragment ions of (a) IPP and (b) ribosylated IPP.
593 The spectra shows similar y”1 and y”2-ions while the presence of m/z 218.2 and m/z 343.2 in (b)
594 revealed that the conjugation occurred at the N-terminus of the tripeptide. Schematic diagram (C)
595 shows the point of fragmentation assigned in figure (B). Also the mass peaks marked with * further
596 supports that the conjugation occurred at the N-terminus. (D) Peak corresponded to *m/z* 211.1 in the
597 mass spectrometry analysis and was assigned as the dehydrated dipeptide IP. The dipeptide was
598 confirmed by the MS/MS analysis on the *m/z* 211.1 and the fragment ions were assigned (D inset).

599

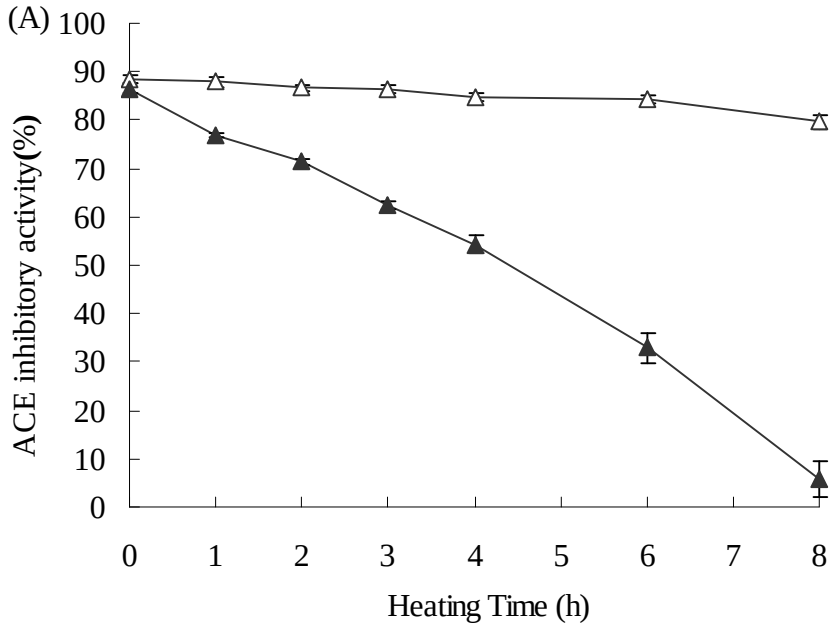

600

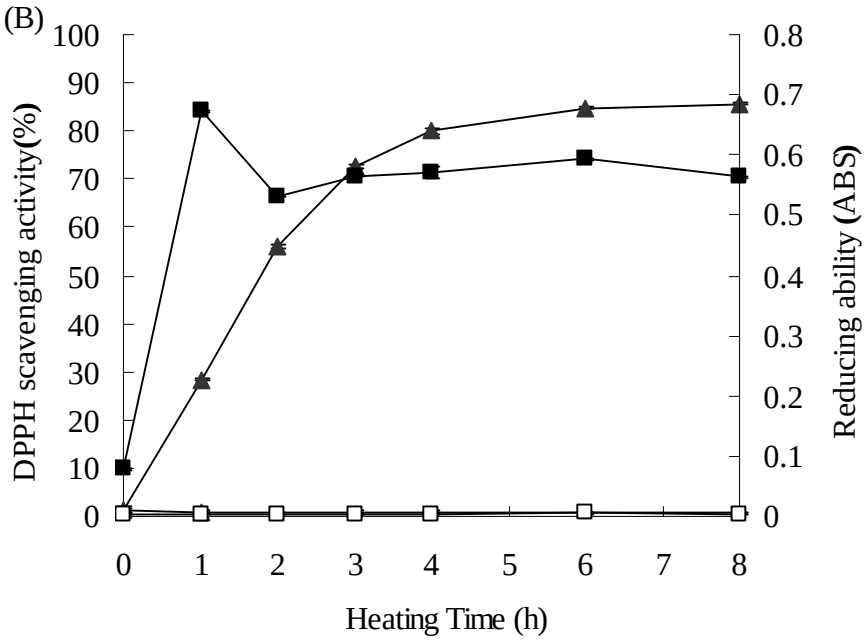

601

602 Fig.5. (A) ACE inhibitory activity during heating of IPP-ribose mixtures (▲) and IPP alone (△). (B)

603 DPPH radical scavenging activity during heating of IPP-ribose mixtures (▲) and IPP alone (△). Ferrous

604 reducing power of IPP-ribose mixtures (■) and IPP alone (□) during heat treatment at 98°C for up to 8

605 hours; Error bars represent the standard deviation of the mean of triplicate experiments.